

See discussions, stats, and author profiles for this publication at: <https://www.researchgate.net/publication/245295224>

Evaluation of Flow Liquefaction and Liquefied Strength Using the Cone Penetration Test

Article in *Journal of Geotechnical and Geoenvironmental Engineering* · June 2010

DOI: 10.1061/(ASCE)GT.1943-5606.0000286

CITATIONS

93

READS

2,863

1 author:



[P. K. Robertson](#)

144 PUBLICATIONS 8,926 CITATIONS

[SEE PROFILE](#)

Some of the authors of this publication are also working on these related projects:



Fraser River Delta Landslide Processes [View project](#)



Quantification of Soil Heterogeneity [View project](#)

Evaluation of Flow Liquefaction and Liquefied Strength Using the Cone Penetration Test

P. K. Robertson¹

Abstract: Flow liquefaction is a major design issue for large soil structures such as mine tailings impoundments and earth dams. If a soil is strain softening in undrained shear and, hence, susceptible to flow liquefaction, an estimate of the resulting liquefied shear strength is required for stability analyses. Many procedures have been published for estimating the residual or liquefied shear strength of cohesionless soils. This paper presents cone penetration test-based relationships to evaluate the susceptibility to strength loss and liquefied shear strength for a wide range of soils. Case-history analyses by a number of investigators are reviewed and used with some additional case histories. Extrapolations beyond the case-history data are guided by laboratory studies and theory.

DOI: 10.1061/(ASCE)GT.1943-5606.0000286

CE Database subject headings: Liquefaction; Cone penetration tests; Soil structures; Case studies; History.

Author keywords: Liquefaction; Strength loss; Cone penetration test; Case histories.

Introduction

Soil liquefaction is a major concern for structures constructed with or on saturated sandy soils. The phenomenon of soil liquefaction has been recognized for many years. Terzaghi and Peck (1967) referred to “spontaneous liquefaction” to describe the sudden loss of strength of very loose sands that caused flow slides due to a slight disturbance. Since 1964, much work has been carried out to explain and understand soil liquefaction. This progress has been described in a series of state-of-the-art papers such as those by Yoshimi et al. (1977), Seed (1979), Finn (1981), Ishihara (1993), Robertson and Fear (1995), Youd et al. (2001), and Robertson (2009c). Much of the work in the past three decades has been on liquefaction induced during earthquake loading (i.e., cyclic liquefaction).

Robertson and Wride (1998) distinguished between liquefaction due to cyclic loading, where the effective overburden stress can reach zero during cyclic loading with a resulting loss of soil stiffness (cyclic liquefaction/softening), and liquefaction due to strain softening with a resulting loss of shear strength (flow liquefaction) and presented a simplified flowchart to aid in the evaluation. Flow liquefaction is also referred to as static liquefaction (e.g., Jefferies and Been 2006). However, since the phenomenon can be triggered by either static or cyclic loading, the term flow liquefaction is used throughout this paper. Flow liquefaction can occur in any saturated or near saturated metastable soil such as very loose cohesionless sands and silts as well as very sensitive clays. For failure of a soil structure, such as a slope or embankment, a sufficient volume of material must strain soften. The re-

sulting failure can be a slide or a flow depending on the material characteristics of the soils and ground geometry. The resulting movements are due to internal, gravity-induced stresses and can occur after the triggering mechanism occurs.

Flow liquefaction is a major design issue for large soil structures such as mine tailings impoundments and earth dams. A liquefaction analysis of sloping ground (i.e., ground subject to a static driving shear stress) is a challenge for geotechnical engineers. Many procedures have been published for estimating the residual or liquefied shear strength of cohesionless soils. Some procedures require a laboratory testing of field samples obtained by ground freezing techniques (e.g., Robertson et al. 2000) or samples obtained by high-quality tube samples coupled with procedures for “correcting” the shear strength for disturbance during sampling and testing (e.g., Castro 1975). However, procedures based on case histories remain the most popular (e.g., Seed 1987; Davis et al. 1988; Seed and Harder 1990; Stark and Mesri 1992; Ishihara 1993; Konrad and Watts 1995; Yoshimine et al. 1999; Olson and Stark 2002; Idriss and Boulanger 2007). Olson and Stark (2002, 2003) suggested a detailed procedure, based on an extensive database of case histories, consisting of three tasks: (1) evaluate susceptibility to strength loss; (2) evaluate liquefied shear strength, $s_{u(liq)}$, and postliquefaction stability; and (3) evaluate if liquefaction will be triggered. Olson and Stark (2002) defined the liquefied shear strength, $s_{u(liq)}$, as the shear strength mobilized at large deformation by a saturated contractive soil following the triggering of a strain-softening response. Others have used the term undrained residual shear strength (e.g., Seed and Harder 1990) or undrained steady-state shear strength (Poulos et al. 1985). The term liquefied shear strength will be used in this paper to be consistent with the more recent Olson and Stark (2002) terminology. The Olson and Stark (2002) procedure uses normalized penetration resistance with no correction for soil type.

Idriss and Boulanger (2007) suggested a correlation to evaluate the liquefied shear strength using an equivalent clean sand normalized penetration resistance. To obtain equivalent clean sand penetration resistance values, Idriss and Boulanger (2007) used the original standard penetration test (SPT)-based correction factors suggested by Seed (1987) and Seed and Harder (1990),

¹Professor Emeritus, Univ. of Alberta, Edmonton, Alberta, Canada; and, Technical Director, Gregg Drilling & Testing, Inc., 2726 Walnut Ave., Signal Hill, CA 90755. E-mail: probertson@greggdrilling.com

Note. This manuscript was submitted on June 2, 2009; approved on November 17, 2009; published online on November 19, 2009. Discussion period open until November 1, 2010; separate discussions must be submitted for individual papers. This paper is part of the *Journal of Geotechnical and Geoenvironmental Engineering*, Vol. 136, No. 6, June 1, 2010. ©ASCE, ISSN 1090-0241/2010/6-842–853/\$25.00.

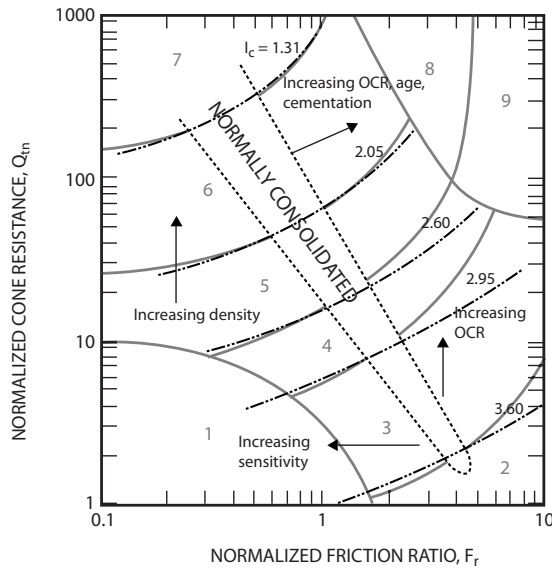


Fig. 1. SBT chart based on normalized CPT parameters (modified from Robertson 1990)

although little justification was provided to support the proposed correction factors. Idriss and Boulanger (2007) also included recommendations regarding potential but undefined void redistribution mechanisms.

Case histories have shown that when significant strength loss occurs in critical sections of a soil structure, failures are often rapid, occur with little warning, and the resulting deformations are often very large. Experience has also shown that the trigger events can be very small. Silvis and de Groot (1995) suggested that triggering should always be assumed if the soils are susceptible to strength loss. Hence, the design for high risk soil structures should be carried out with caution. In general the emphasis in design is primarily on the evaluation of susceptibility to strength loss and the resulting liquefied shear strength.

This paper presents cone penetration test (CPT)-based relationships to evaluate the susceptibility to strength loss and liquefied shear strength for a wide range of soils. Case-history analyses by a number of investigators are reviewed and used with some additional newer case histories. Emphasis is placed on more recent case histories that had modern CPT measurements available. Extrapolations beyond the case-history data are guided by laboratory studies and theory.

Normalized CPT Parameters

Robertson (1990) developed a chart to identify soil behavior type (SBT) based on normalized CPT parameters as shown in Fig. 1. The CPT parameters are normalized by the effective overburden stress to produce dimensionless parameters, Q_t and F_r , where

$$Q_t = (q_t - \sigma_{vo}) / \sigma'_{vo} \quad (1)$$

$$F_r = [f_s / (q_t - \sigma_{vo})] 100\% \quad (2)$$

where q_t = CPT corrected total cone resistance (Campanella et al. 1982); f_s = CPT sleeve friction; σ_{vo} = preinsertion in situ total vertical stress; and σ'_{vo} = preinsertion in situ effective vertical stress.

Jefferies and Davies (1993) identified that a SBT index, I_c , could represent the SBT zones in the Q_t - F_r chart where I_c is

essentially the radius of concentric circles that define the boundaries of soil type. Robertson and Wride (1998) modified the definition of I_c to apply to the Robertson (1990) Q_t - F_r chart as defined by

$$I_c = [(3.47 - \log Q_t)^2 + (\log F_r + 1.22)^2]^{0.5} \quad (3)$$

Robertson and Wride (1998), as updated by Robertson (1999) and Zhang et al. (2002), suggested a normalized cone parameter to evaluate soil liquefaction, using normalization with a variable stress exponent, n , where

$$Q_m = [(q_t - \sigma_{vo}) / p_a] (p_a / \sigma'_{vo})^n \quad (4)$$

where $(q_t - \sigma_{vo}) / p_a$ = dimensionless net cone resistance; $(p_a / \sigma'_{vo})^n$ = stress normalization factor; n = stress exponent that varies with SBT; and p_a = atmospheric pressure in the same units as q_t and σ_{vo} .

Note that when $n=1$, $Q_m = Q_t$. Zhang et al. (2002) suggested that the stress exponent, n , could be estimated using the SBT index, I_c , and that I_c should be defined using Q_m . Contours of I_c are included in Fig. 1 to illustrate the trend.

In recent years there have been several publications regarding the appropriate stress normalization (Olsen and Malone 1988; Robertson 1999; Zhang et al. 2002; Idriss and Boulanger 2004; Moss et al. 2006; Cetin and Isik 2007). All the methods agree that in the clean sand region of the Q_m - F_r SBT chart (Zone 6) the stress exponent is typically close to 0.5 and in the clay region of the SBT chart (Zone 3) the stress exponent is close to 1.0. Only the normalized SBT chart suggested by Jefferies and Davies (1991) uses a stress normalization of $n=1.0$ throughout. Robertson (2009b) provided a detailed discussion on stress normalization and suggested the following updated approach to allow for a variation of the stress exponent with both SBT I_c (soil type) and stress level using

$$n = 0.381(I_c) + 0.05(\sigma'_{vo} / p_a) - 0.15 \quad (5)$$

where $n \leq 1.0$.

Robertson (2009b) suggested that the above stress exponent would capture the correct in situ state for soils at high stress level and that this would also avoid any additional stress level correction for liquefaction analyses. It is well recognized that the normalized cone resistance decreases as a soil becomes more fine grained due to the increasing compressibility of fine-grained soils compared to coarse-grained soils. This was identified by Robertson (1990) where the normally consolidated region on the CPT SBT chart extends down the chart; i.e., as soil becomes more fine grained the normalized cone resistance (Q_m) decreases and F_r increases. Robertson and Wride (1998) suggested that the soil behavior index I_c increases when soils become more fine grained and that when $I_c > 2.60$ soils tend to be more claylike. Independent studies (Gilstrap and Youd 1998; Cetin and Ozan 2009; Robertson 2009a) have confirmed that most samples are claylike when $I_c > 2.60$.

Robertson (2009b) updated the trends in normalized cone parameters with overconsolidation ratio (OCR), sensitivity (S_r), and age as shown in Fig. 1. In fine-grained soils, the normalized cone resistance (Q_m) increases with increasing OCR with little influence on the normalized friction ratio (F_r). On the other hand, F_r decreases with increasing S_r , with little influence on Q_m . Both Q_m and F_r tend to increase as soils become stiffer and stronger with age.

Table 1. Case Histories of Flow Liquefaction Failures with Measured or Estimated Penetration Resistance > Values

Case history				Soil data		CPT mean values			
Number ^a	Structure	Available data	Class	Approximate D_{50} (mm) ^a	Approximate FC (%) ^a	Q_{in}	F_r (%)	I_c	$Q_{in,cs}$
1	Zeeland	MCPT	B	0.12	3–11	30	0.25	2.1	43
2	Wachusett Dam	SPT	C	0.42	5–10	46	0.60	2.1	64
3	Calaveras Dam	D_R	D	—	10 to >60	50	1.0	2.2	77
4	Sheffield Dam	D_R	D	0.10	33–48	22	1.0	2.4	56
5	Helsinki Harbor	Estimate	E	—	—	40	—	—	—
6	Fort Peck Dam	SPT	C	0.06–0.20	~55	18	1.5	2.6	62
7	Solfatara Canal	D_R	D	0.17	6–8	25	0.6	2.3	49
8	Lake Merced bank	D_R , SPT	C	0.21 (0.18–0.25)	1–4	32	0.5	2.2	51
9	Kawagishi-Cho Building	MCPT, SPT	B	0.35	<5	31	0.5	2.2	50
10	Uetsu Railway embankment	Estimate	E	0.30–0.40	0–2	18	0.2	2.2	34
11	El Cobre Tailing Dam	SPT	C	0.08 to unknown	55–93	~3	2.0–5.0	3.0–3.5	40
12	Koda Numa embankment	Estimate	E	0.15–0.20	~13	13.5	0.7	2.6	42
13	Metoki Road embankment	Estimate	E	Silty sand	—	10.5	0.4	2.6	34
14	Hokkaido Tailings Dam	MCPT	B	~0.074	~50	4.0	1.0–2.0	3.2	36
15	LSFD	CPT, SPT	A	~0.074 (0.02–0.30)	~50 (5–90)	Silt: 5	3.5	3.3	52
16	Tar Island Tailings	SPT	C	~0.15	~10–15	30	0.6	2.2	52
17	Mochi-Koshi Tailings Dike 1	MCPT, SPT	B	0.04	85	5.0	2.0–3.0	3.3	48
18	Mochi-Koshi Tailings Dike 2	MCPT, SPT	B	0.04	85	5.0	2.0–3.0	3.3	48
19,20,21	Nerlerk 1, 2, and 3	CPT	A	0.22	2–12	40	0.4	2.0	55
22	Hachiro-Gata Road	MCPT, SPT	B	0.20	10–20	30	0.5	2.2	50
23	Asele Road	SPT	C	0.30 (0.15–0.55)	32 (23–38)	30	1.5	2.4	74
24	La Marquesa Dam U/S slope	SPT	C	~0.15	~30	20	1.0	2.5	54
25	La Marquesa Dam D/S slope	SPT	C	~0.15	~20	30	0.5	2.2	50
26	La Palma Dam	SPT	C	~0.20	~15	18	0.5	2.3	41
27	Fraser River Delta	CPT	A	0.25	0–5	15	1.5	2.6	58
28	Lake Ackerman embankment	SPT	C	0.40	0	19	0.5	2.4	42
29	Chonan Middle School	SPT	C	~0.20	18	26	0.6	2.3	50
30	Nalband Railway embankment	SPT	C	~1.50	~20	60	0.4	1.9	70
31	Soviet Tajik	MCPT	B	0.012	100	19	1.0	2.6	53
32	Shibecha-Cho embankment	Estimate	E	0.20 (0.12–0.40)	20 (12–35)	28	0.6	2.3	51
33	Route 272 at Higashiarekinai	SPT	C	~0.20	20	32	0.6	2.2	53
34	Jamuna Bridge	CPT	A	~0.20	~10	30	0.8	2.2	57
35	Sullivan Tailings	CPT	A	~0.075	~50	15	1.0	2.6	50
36	Canadian Mine	CPT	A	~0.020	100	6	1.0	3.0	38

Note: Available data (based on Olson and Stark 2002): Estimate=no measurements made; values estimated; D_R =relative density estimates; SPT=standard penetration test; MCPT=mechanical cone penetration test; CPT=electric cone penetration test.

^aFrom Olson and Stark (2002).

Case Histories

Olson (2001) and Olson and Stark (2002) presented a comprehensive summary of case histories where flow liquefaction occurred. Table 1 contains an updated summary of the case histories presented by Olson and Stark (2002). Most of the case histories presented by Olson and Stark (2002) did not have detailed CPT records that included sleeve friction measurements. However, there are six (6) case histories where flow liquefaction occurred and where detailed electric CPT records are available (the three Nerlerk berm failures are combined). Three of these case histories were included in the Olson and Stark (2002) summary. The additional three new case histories, that were not part of the Olson and Stark (2002) study, have been added at the end of Table 1. The three additional new case histories are Jamuna Bridge, Sullivan Tailings, and Canadian Mine. Details about the Jamuna Bridge case can be found in Ishihara (1993) and Yoshimine et al. (1999)

and the Sullivan Tailings in Davies et al. (1998) and Jefferies and Been (2006). The Canadian Mine case history comes from the personal files of the writer and will be briefly described here.

During the preliminary design stage for a proposed open-pit mine in Canada, a trial excavation was made to evaluate the stability of the natural surface soils. The surface soils in one region were primarily composed of soft, low plastic, sensitive silty clay extending to a depth of about 10–15 m. The silty clay had an average plasticity index (PI) of about 8 with a high liquidity index (LI) of about 1.2. The high LI is consistent with the high sensitivity (Leroueil et al. 1983) and low residual/liquefied shear strength. During the excavation, a 50-m-wide flow failure occurred within the sensitive clay in a 5-m-high, 50-degree bench slope. The upper 2.5 m of soil was frozen. The flow slide was retrogressive in nature and the failed soil moved into the excavation along an almost horizontal surface. The size of failed mass almost doubled in size over a 4-day period.

The six case-history sites where CPT measurements were available (including sleeve friction values) are identified in Table 1 as Class A, since they are the most reliable in terms of CPT data. Four of the more recent Class A case histories had CPT measurements prior to the failure. Some older case histories had either mechanical CPT (MCPT) or electric CPT but no friction sleeve values and are identified as Class B. Class B results are less reliable than Class A records in terms of the CPT data. Other case histories used values estimated by Olson (2001) from either SPT, relative density, or best estimates and are identified as either Class C, Class D, or Class E, respectively. Table 1 illustrates that many of the older case histories had very little available data on which to estimate an equivalent CPT. Classes C, D, and E are not reliable in terms of CPT results, since no CPT measurements were made. Table 1 follows the same numbering system used by Olson and Stark (2002) and contains the basic information on approximate mean grain size (D_{50}) and fines content (FC) of the soil involved in the failure.

One of the challenges when reviewing case-history records is the evaluation of representative in situ test values. Even in relatively uniform deposits of sand, the normalized cone resistance can vary over a wide range. Soil variability in terms of soil type also complicates the process in interlayered deposits. Often an average or mean CPT value within the zone that is estimated to have been involved in the slide is used. Popescu et al. (1997) suggested that the 20-percentile value would be more appropriate, since the weaker zones control instability. The 20-percentile value is defined as the value at which 20% of the measured values are smaller (i.e., 80% are larger). Whatever criterion is selected, the resulting correlations are often applied to every measured CPT data point, typically every 50 mm.

Olson (2001) and Jefferies and Been (2006) provided details for the case histories that will not be repeated here. The only case history that requires some further description is the Lower San Fernando Dam (LSFD), since it illustrates the challenge in selecting an appropriate representative penetration resistance in highly interlayered deposits.

LSFD

A major slide occurred in the upstream slope of the 43-m-high LSFD following the 1972 San Fernando earthquake ($M_w \sim 6.6$). A number of major studies have documented this case history, e.g., Seed et al. (1973), Castro et al. (1989), Seed et al. (1989), and numerous investigators have analyzed the slide, e.g., Davis et al. (1988), Seed and Harder (1990), Castro et al. (1992), and Olson (2001). The LSFD is one of the most studied liquefaction flow slides in the literature.

The zone of soil that experienced strength loss was within the lower sections of the upstream hydraulic fill and close to the central “core” (Castro et al. 1992). Large blocks of intact embankment material moved into the reservoir, “floating” on the remolded/liquefied soil. The slide occurred between 20 and 40 s after the earthquake shaking had stopped.

The dam site is underlain by stiff clay with layers of sand and gravel. The majority of the dam consists of hydraulic fill placed between 1912 and 1915. The hydraulic fill was sluiced from the reservoir area and placed from upstream and downstream starter dams. The grain size distribution curves for the hydraulic fill show a FC ranging from 20 to 90%. Two CPT profiles obtained in 1985 from the center of the downstream slope (C103 and C104) are shown in Fig. 2 in terms of normalized penetration resistance, Q_{tn} . These CPT profiles were selected because they were located

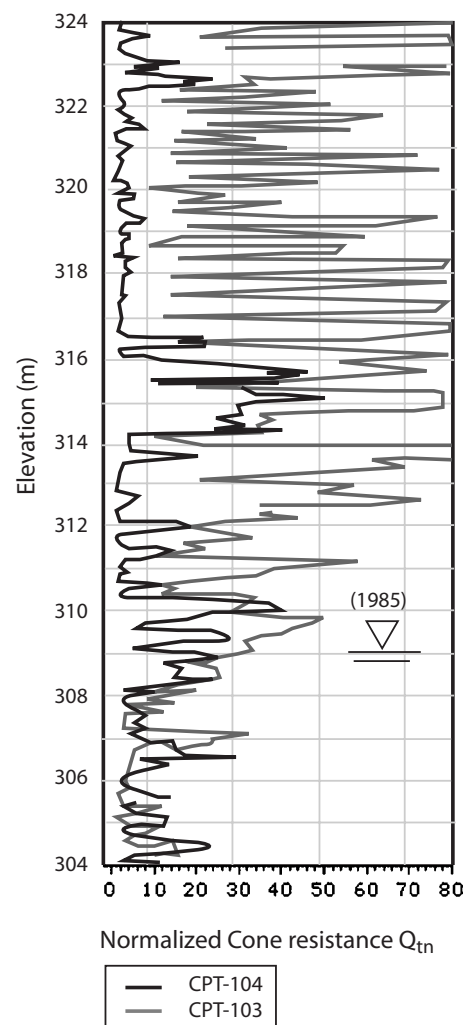


Fig. 2. LSFD CPT profiles (C103 and C104)

in the center of the downstream hydraulic fill shell of the LSFD and appear to best represent the expected soils in the failure region of the upstream slope (Castro et al. 1989; Jefferies and Been 2006). C103 was started at an elevation of about 334 m and was downstream of C104, which was started at an elevation of about 340 m. The groundwater at the time of the CPT in 1985 was at an elevation of about 309 m. A cross section of the dam was presented by Idriss and Boulanger (2007) that showed the relative locations of the CPT profiles. Although most published cross sections of the LSFD show a well defined “clayey puddle core” supported by an adjacent “hydraulic fill shell,” it is likely the hydraulically placed fill progressively grades from predominately coarse-grained to predominately fine-grained soils toward the central area of the dam with frequent interlayering due to changes in source location. Above elevation of 324 m the soils were dense sand fill. Fig. 2 shows that below elevation of 324 m the CPTs show a variable interlayered hydraulic fill that ranges from sand to sandy silt. The highly interlayered nature of the soil is common for hydraulically placed fills. Below an elevation of 324 m, C104 is composed mostly of loose sandy silt with some sand layers at depth whereas C103 is composed of interlayered sand and sandy silt down to an elevation of 308 m. Between elevations of 305–308 m in C103 the soil is predominately sandy silt to silt. Laboratory tests on samples confirmed that the fine-grained portions are low to nonplastic sandy silt to silt (Castro et al. 1992).

The zone of soil that experienced strength loss was within the lower sections of the upstream hydraulic fill between approximate elevations of 305–315 m. The selection of a representative penetration resistance is difficult since the failed soil in the upstream slope was no longer available for testing and assumptions were made regarding the similarity between upstream and downstream soil profiles. Previous studies have typically selected a single “representative” penetration resistance value as the average value for the interlayered sand and silt. For example, Olson and Stark (2002) selected a normalized cone resistance of 47 which is not representative of either the silt or the sand. The CPT profiles clearly show that the deposit is made up of two interlayered soils; sand and sandy silt to silt. The amount of silt increases toward the center of the dam due to the direction of hydraulic deposition. The largest zone that was considered to have experienced strength loss was close to the central core of the dam. In C104, below an elevation of 315 m, the sand layers are generally too thin to obtain representative penetration resistance values (Ahmadi and Robertson 2005). In C103, below an elevation of 315 m, only the sand layer from about elevations of 308.8–310.2 m appears to be sufficiently thick to obtain a representative penetration resistance value within the sand. The lower penetration resistance values in both profiles are more representative of the loose sandy silt to silt. The representative normalized penetration resistance within the sandy silt to silt is significantly smaller than within the sand. Jefferies and Been (2006) discussed in detail the interpretation of the CPT at the LSFD and concluded that the in situ state of the sandy silt to silt was significantly weaker than the in situ state of the sand. The CPT also indicates that the sandy silt to silt has a sensitivity of about 2 or more based on the relatively low friction ratio values (Robertson 2009b). It is likely that the sandy silt to silt experienced high pore pressures during the earthquake which resulted in postearthquake strength loss. Applying the CPT-based approach for the cyclic liquefaction method recommended by Youd et al. (2001) and updated by Robertson (2009b) for $a_{\max} = 0.5$ g, the sandy silt to silt is predicted to have experienced cyclic softening with significantly higher pore pressures than the sand layers. There is no clear evidence that strength loss occurred in the thin sand layers. In this study, only the representative penetration resistance value for the loose sandy silt to silt has been used for the LSFD case history. This approach was also supported by the detailed analyses carried out by Jefferies and Been (2006). The LSFD is the only Class A (and Class B) case history that involves highly interlayered soils. Shuttle and Cuning (2007) presented CPT results for a nonplastic hydraulically placed silt that had normalized CPT values very similar to those found in the LSFD silt and confirmed a potential for strength loss.

Included in Table 1 are the best estimates of the mean values of normalized CPT parameters based on the information available from the literature. The estimated CPT values for the case histories where no CPT data were available (i.e., Classes C, D, and E) are approximate at best and less reliable than those where modern electric CPT measurements (Class A) were made. The estimated normalized cone resistance (Q_m) values (for Classes B, C, D, and E) were based on the values selected by Olson and Stark (2002). The estimated values of F_r and I_c were based on the estimated values of Q_m , soil description, and available soil characteristics provided by Olson (2001) and the relationship between I_c and FC suggested by Robertson and Wride (1998). The estimated CPT values for the case histories where no CPT measurements were available are clearly approximate and subject to considerable judgment and uncertainty. Hence, the subsequent analysis is based primarily on the six main case histories where complete

CPT measurements were available (i.e., Class A) with support from the Class B cases, which were mostly simple mechanical CPT. The Classes C, D, and E case histories are presented only for completeness, since they were part of the original Olson and Stark (2002) database, but were not used to define recommended criteria.

It is interesting to note that all the soils involved in the case-history flow liquefaction failures shown in Table 1 were young (<10,000 years), with 83% less than 50 years and 33% less than 10 years. The Canadian Mine case history is the only case history included in Table 1 that involves a natural sensitive silty clay, although there have been other observed flow failures in very sensitive “quick clays” (e.g., Rissa landslide of 1978). Most of the soils involved in the failures in Table 1 were either nonplastic or had low plasticity; 78% were fills; 39% were hydraulically placed; and 16% were mine tailings. About 50% of the failures were triggered by earthquake loading. Several failures were triggered by very minor disturbances (e.g., Nerlerk, Fraser River, and Jamuna).

The case histories indicate that very young, very loose, nonplastic or low-plastic soils tend to be more susceptible to significant and rapid strength loss than older, denser, and/or more plastic soils. Although some plastic clays can have high sensitivity (i.e., significant strength loss when sheared undrained), they are typically more ductile than very loose, nonplastic or low-plastic soils and tend to reach peak and remolded shear strength at large shear strains (Ladd et al. 1977). A feature of the sensitive fine-grained soils that exist in flow failures is their relatively low plastic limit and small shear strain to peak undrained shear strength (Leroueil and Hight 2003).

Evaluate Susceptibility to Flow Liquefaction

Since flow liquefaction requires a strain-softening soil response and strength loss, the evaluation of susceptibility to flow liquefaction is controlled by an evaluation of the potential for a soil to strain soften in undrained shear. Experience has shown that very loose sands and very sensitive low-PI clays can experience an abrupt loss of strength at small shear strains resulting in low undrained shear strength. Although many natural high-PI clays can also experience some strength loss, they tend to be more ductile and experience more gradual loss of strength at larger shear strains. Cohesive soils with a shear strain to peak undrained strength greater than about 5% and a gradual drop-off in resistance after reaching the peak strength are less likely to experience flow liquefaction. Hence, the key element to identify a soil's susceptibility to flow liquefaction is to identify very loose coarse-grained soils (i.e., sand, silty sands, and sandy silts) and very sensitive fine-grained soils (silts, silty clays, clayey silts, and clays).

The concepts for strength loss and liquefied shear strength in sands stem from the work on the critical void ratio by Casagrande (1940). Castro (1969) expanded the basic concept of a critical void ratio and developed the term steady state to define the liquefied strength. At about the same time, the concepts of critical state soil mechanics were under development in the U.K. by Schofield and Wroth (1968). Both concepts recognize that the state of a soil is represented by a combination of the void ratio and effective stress and that if a soil is loose of either steady or critical state the soil can strain soften in undrained shear.

Been and Jefferies (1985) used critical state soil mechanics to develop the state parameter (ψ) concept and applied these con-

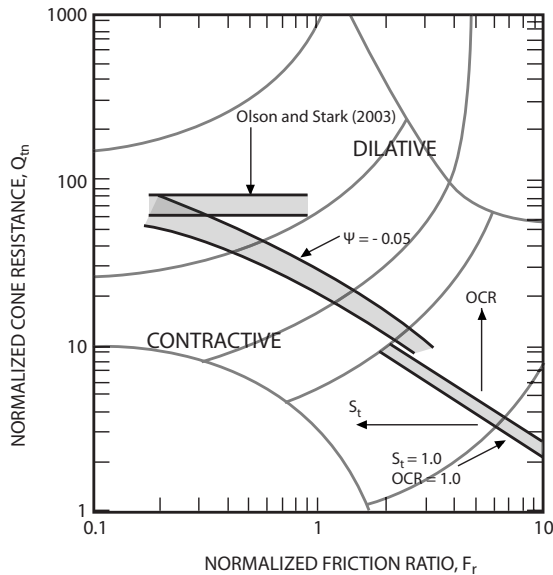


Fig. 3. Approximate boundary between dilative and contractive soil response using normalized CPT parameters

cepts to the CPT results (Been et al. 1986) and to soil liquefaction (Jefferies and Been 2006). The state parameter (ψ) is defined as the difference between the in situ void ratio, e_o , and the void ratio at critical state, e_{cs} , at the same mean effective stress, p' (Been and Jefferies 1985). Jefferies and Been (2006) provided a detailed description of the evaluation of the soil state using the CPT and show that the inverse problem of evaluating the state from the CPT response is complex and depends on several soil parameters. For high risk projects, a detailed interpretation of the CPT results using laboratory results and numerical modeling can be appropriate (e.g., Shuttle and Cuning 2007), although soil variability can complicate the interpretation procedure.

For low risk projects and in the initial screening for high risk projects, it is often appropriate to estimate the state of the soil directly from the CPT results. Plewes et al. (1992) developed a screening method to estimate the state of the soil using the normalized CPT results. This was subsequently updated and modified by Jefferies and Been (2006). In a general sense, soils with a state denser than the critical state ($\psi < 0$) will be dilative and will strain harden in undrained shear, whereas soils with a state looser than the critical state ($\psi > 0$) will be contractive and will strain soften in undrained shear. Jefferies and Been (2006) and Shuttle and Cuning (2007) suggested that when a soil has a state parameter $\psi > -0.05$, strain softening and strength loss in undrained shear can be expected. Hence, defining a region on the CPT SBT chart that represents a state parameter of about -0.05 is helpful as a screening technique to identify the susceptibility for flow liquefaction.

Based on the work of Plewes et al. (1992), Jefferies and Been (2006), and Shuttle and Cuning (2007), combined with the test results from frozen samples (Robertson et al. 2000), it is possible to identify a zone on the normalized SBT, based on Q_m and F_r , that represents the approximate boundary between the dilative and contractive soil response as shown in Fig. 3. Also identified in Fig. 3 is the region that defines normally consolidated clays with a sensitivity of 1 or more based on the work of Robertson (2009b). Robertson (2009b) showed that as the soil sensitivity increases in fine-grained soils, the measured CPT normalized friction ratio (F_r) decreases as indicated in Fig. 3. As shown by

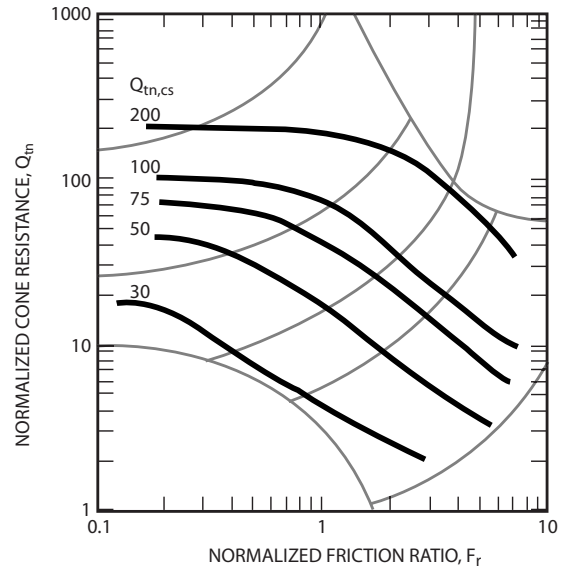


Fig. 4. Contours of equivalent clean sand normalized cone resistance, $Q_{m,cs}$, based on corrections suggested by Robertson and Wride (1998)

Plewes et al. (1992) and Jefferies and Been (2006) and illustrated in Fig. 3, there is a clear trend for the normalized cone resistance to decrease as I_c increases for the same soil state. Fig. 3 indicates that the region in the lower left portion of the SBT chart defines soils that are likely susceptible to contractive behavior and strength loss in undrained shear. Included in Fig. 3 is the approximate boundary between the contractive and dilative soil response suggested by Olson and Stark (2003) based on the normalized penetration resistance. The Olson and Stark (2003) criteria vary slightly with effective overburden stress and a range is presented. It is clear from Fig. 3 that the criterion suggested by Olson and Stark (2003) applies only to clean sands where typically $F_r < 1\%$.

Robertson and Wride (1998) suggested a correction factor to correct the normalized cone resistance in silty sands to an equivalent clean sand value ($Q_{m,cs}$) using the following:

$$Q_{m,cs} = K_c Q_{m,cs} \quad (6)$$

where K_c = a correction factor that is a function of grain characteristics (combined influence of FC, mineralogy, and plasticity) of the soil that can be estimated using I_c as follows:

$$K_c = 1.0 \text{ if } I_c \leq 1.64 \quad (7)$$

$$K_c = 5.581I_c^3 - 0.403I_c^4 - 21.63I_c^2 + 33.75I_c - 17.88 \text{ if } I_c > 1.64 \quad (8)$$

Fig. 4 shows the contours of the equivalent clean sand cone resistance, $Q_{m,cs}$, on the CPT SBT chart. The contours of $Q_{m,cs}$ follow a trend similar to the dilative-contractive boundary defined in Fig. 3 and that a value of $Q_{m,cs}$ between 50 and 70 likely represents the boundary between the contractive and dilative state for a wide range of soils. Robertson (2010) indicated that the contours of $Q_{m,cs}$ are essentially contours of the state parameter (ψ). Hence, soils with a constant value of $Q_{m,cs}$ have essentially a similar state parameter and hence a similar response to loading. Although the concept of an equivalent clean sand penetration resistance stems from the early work of Seed (1979), based on a "FC correction," Jefferies and Been (2006) showed that a correc-

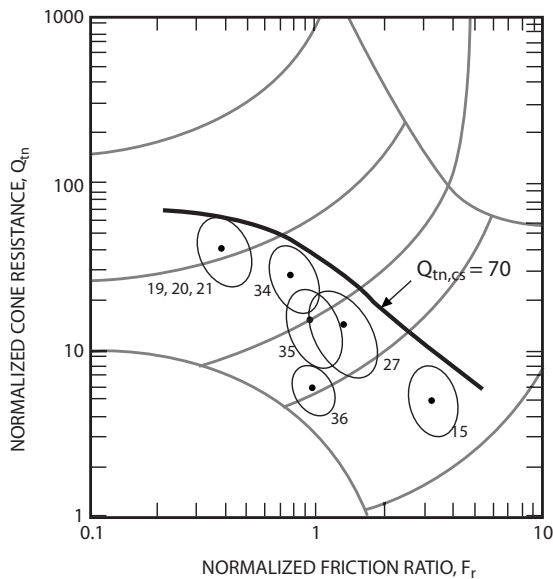


Fig. 5. Range (mean and standard deviation) of normalized CPT data from Class A flow liquefaction failure case histories (numbers represent case histories from Table 1)

tion based on the slope of the critical state line (λ) is essentially similar but conceptually more correct. Jefferies and Been (2006) also showed that λ was a function of the CPT SBT index (I_c). Hence, the equivalent clean sand cone resistance approach using a correction based on I_c , as suggested by Robertson and Wride (1998), is supported, in a general sense, by the theoretical approach described by Jefferies and Been (2006) based on critical state soil mechanics.

Fig. 5 presents the CPT data from the six Class A case histories in terms of measured normalized cone results on the normalized CPT-based SBT chart. The CPT data shown in Fig. 5 represent approximately the mean ± 1 standard deviation values within the zone that was considered to have experienced strength loss and involved in the slide. The data within ± 1 standard deviation represent about 68% of the data (i.e., approximately 16% is smaller and 16% larger). The measured CPT results from each case history represent a region on the normalized SBT chart that illustrate the variation in CPT values within each deposit that experienced strength loss. The mean value would represent approximately the center of each region and the 20-percentile value would be approximately the lower right portion of each region of data for a case history. Also included in Fig. 5 is a contour that represents a clean sand equivalent penetration resistance, $Q_{m,cs} = 70$. The contour of $Q_{m,cs} \leq 70$ captures all the CPT results defined by the mean+1 standard deviation (i.e., about 70% of the results within the deposit) for the Class A case histories.

Several flow liquefaction failures have also been documented in the quick clays found in Norway and eastern Canada (e.g., Rissa landslide of 1978). These “quick clays” have normalized CPT values in the region of $Q_m < 10$ and $F_r < 2\%$ (Lunne et al. 1997) similar to the sensitive silty clay found at the Canadian Mine case history (No. 36, Table 1). Hence, the flow liquefaction failures in quick clay also plot within the region defined by the contour $Q_{m,cs} \leq 70$.

Fig. 6 presents the mean values for all the case histories, but the six cases where full CPT measurements were available (Class A) are represented with solid symbols; Class B by the large shaded symbols; and the less reliable estimated values (Classes C,

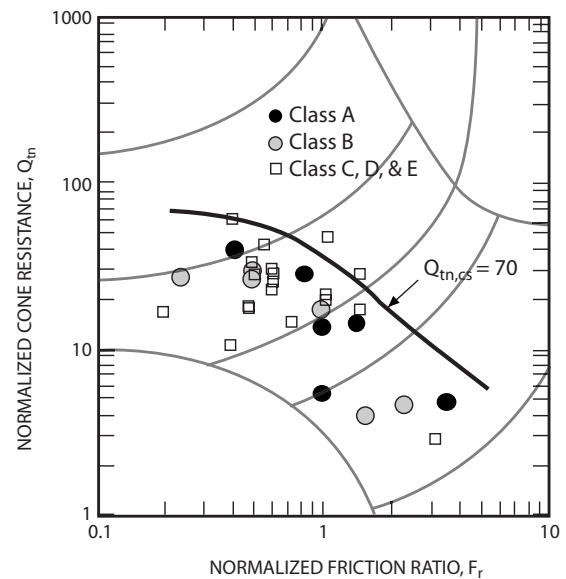


Fig. 6. Mean values of normalized CPT data from flow liquefaction failure case histories

D, and E) are represented with small open symbols. The contour of $Q_{m,cs} = 70$ captures the case-history records reasonably well and captures the change in the CPT response as soils vary from clean sands to soft sensitive clays and silts. Any small variation in the estimated values of F_r and I_c for the Classes C, D, and E case histories using the Q_m values selected by Olson (2001) would have little influence on the overall observation. Soils with a $Q_{m,cs} > 70$ are likely dilative and strain hardening in undrained shear consistent with the state parameter approach described by Jefferies and Been (2006). Hence, the criteria of $Q_{m,cs} \leq 70$ can be used as a conservative screening method to evaluate if a soil is susceptible to strain softening in undrained shear and, hence, susceptible to flow liquefaction.

Evaluation of Liquefied Shear Strength

Estimating liquefied shear strength values ($s_{u(liq)}$) from failure case histories uses stability calculations that require many simplifying assumptions and idealizations. Most approaches use limit equilibrium methods based on either prefailure or postfailure geometry and may or may not include inertial effects. Many case histories involved retrogressive sliding that is rarely accounted for in the back-analyses. Hence, the evaluation of the liquefied shear strength based on case histories is often approximate at best. Many researchers (e.g., Seed 1987; Seed and Harder 1990; Wride et al. 1999; Olson and Stark 2002; Jefferies and Been 2006) have estimated the shear strength of liquefied soils based on case histories. Jefferies and Been (2006) showed that there is a theoretical link between the state parameter and the liquefied undrained shear strength ratio ($s_{u(liq)}/\sigma'_{vo}$). Since clean sand equivalent normalized penetration resistance ($Q_{m,cs}$) is essentially equivalent to the state parameter, values of $Q_{m,cs}$ are compared to $s_{u(liq)}/\sigma'_{vo}$ for the case histories, with emphasis on the Class A case histories. The range of published estimated $s_{u(liq)}/\sigma'_{vo}$ values for the case histories is presented in Table 2 using the same numbering system as shown in Table 1. Olson and Stark (2002) and Olson (2001) described the sources of uncertainty in the analyses and their relative importance. Some case histories have a wide range of estimated

Table 2. Case Histories of Flow Liquefaction Failures with Published Estimated Liquefied Shear Strength Ratio Values

Number ^a	Structure	Liquefied strength ratio					Best estimate	Class
		Seed (1987)	Seed and Harder (1990)	Wride et al. (1999)	Olson and Stark (2002)	Jefferies and Been (2006)		
1	Zeeland	—	—	—	0.048	0.130	0.05	B
2	Wachusett Dam	—	—	—	0.106 ^b	0.07–0.13	0.11	C
3	Calaveras Dam	0.117	0.101	0.246	0.112 ^b	0.31–0.35	0.11	D
4	Sheffield Dam	0.035	0.053	0.038	0.053	0.04–0.07	0.05	D
5	Helsinki Harbor	—	—	—	0.060	—	0.06	E
6	Fort Peck Dam	0.082	0.048	0.065	0.078 ^b	0.04–0.06	0.08	C
7	Solfatara Canal	0.208	0.080	0.052	0.080	—	0.08	D
8	Lake Merced bank	0.073	0.073	0.107	0.108	—	0.11	C
9	Kawagishi-Cho Building	0.081	0.081	0.097	0.075	—	0.08	B
10	Uetsu Railway embankment	0.027	0.031	0.029	0.027	—	0.03	E
11	El Cobre Tailing Dam	—	—	—	0.020	—	0.02	C
12	Koda Numa Highway embankment	0.103	0.103	0.032	0.052 ^b	—	0.05	E
13	Metoki Road embankment	—	—	—	0.043	—	0.04	E
14	Hokkaido Tailings Dam	—	—	—	0.073	0.08–0.12	0.10	B
15	LSFD	0.215	0.115	0.127	0.112 ^b	0.07–0.12	0.11	A
16	Tar Island Dyke	—	—	—	0.058	—	0.06	C
17	Mochi-Koshi Tailings Dike 1	—	—	0.048	0.060	0.08	0.06	B
18	Mochi-Koshi Tailings Dike 2	0.229	0.229	0.024	0.104	0.14–0.16	0.10	B
19,20,21	Nerlerk 1, 2, and 3	—	—	—	0.034–0.086	0.09–0.15	0.09	A
22	Hachiro-Gata Road	—	—	—	0.062 ^b	—	0.06	B
23	Asele Road	—	—	—	0.104	—	0.10	C
24	La Marquesa Dam U/S slope	—	0.220	0.125	0.070	0.08–0.10	0.07	C
25	La Marquesa Dam D/S slope	—	0.400	0.223	0.110	0.08–0.10	0.11	C
26	La Palma Dam	—	0.253	0.120	0.120	0.12–0.15	0.12	C
27	Fraser River Delta	—	—	—	0.100	—	0.10	A
28	Lake Ackerman embankment	—	—	0.117	0.076 ^b	—	0.08	C
29	Chonan Middle School	—	—	—	0.091	—	0.09	C
30	Nalband Railway embankment	—	—	—	0.109	—	0.11	C
31	Soviet Tajik	—	—	—	0.082	—	0.08	B
32	Shibecha-Cho embankment	—	—	—	0.086 ^b	—	0.09	E
33	Route 272 at Higashiarekinai	—	—	—	0.097 ^b	—	0.10	C
34	Jamuna Bridge	—	—	—	—	0.12–0.20	0.15	A
35	Sullivan Tailings	—	—	—	—	0.07–0.13	0.10	A
36	Canadian Mine	—	—	—	—	—	0.06	A

^aFrom Olson and Stark (2002).^bValues that consider the kinetics of failure.

back-calculated shear strength values (Table 2). Olson and Stark (2002) performed stability analyses considering kinetics of the failure mass on 10 case histories, where this was possible, and these are identified in Table 2. When kinetics is considered, the back-calculated shear strength values were larger than if kinetics were not included. The Olson and Stark (2002) values used a weighted average prefailure vertical effective stress to estimate the liquefied shear strength ratio. The strength ratio values under Seed (1987) and Seed and Harder (1990) were also computed using the same average values of prefailure vertical effective stress. Based on a review of the published values and placing emphasis on the values computed by Olson and Stark (2002), “best estimate” values for the liquefied shear strength are assigned for each case history and are included in Table 2. Previous studies have presented back-calculated values of the liquefied shear strength ratios to three decimal places. This level of perceived accuracy is inconsistent with the many uncertainties in the back-

calculation of flow slides and this study has shown “best estimated” values to only two decimal places. For consistency the best estimate values (for the cases in the Olson and Stark 2002 database) are the same as those computed by Olson and Stark (2002), but rounded to two decimal places. Olson and Stark (2002) treated the Nerlerk case as three separate slides with a range of back-calculated values. This study has combined the slides into one case and assigned a value close to the higher value back-calculated by Olson and Stark (2002), but equal to the lower value of the range suggested by Jefferies and Been (2006). The values selected for the three newer cases (that were not in the Olson and Stark 2002 database) were the average values suggested by Jefferies and Been (2006) for Cases Nos. 34 and 35 and the value back-calculated by the writer for the new Case No. 36. The values suggested by others are presented in Table 2 to illustrate the possible range in back-calculated values.

When soils are strain hardening in undrained shear, the un-

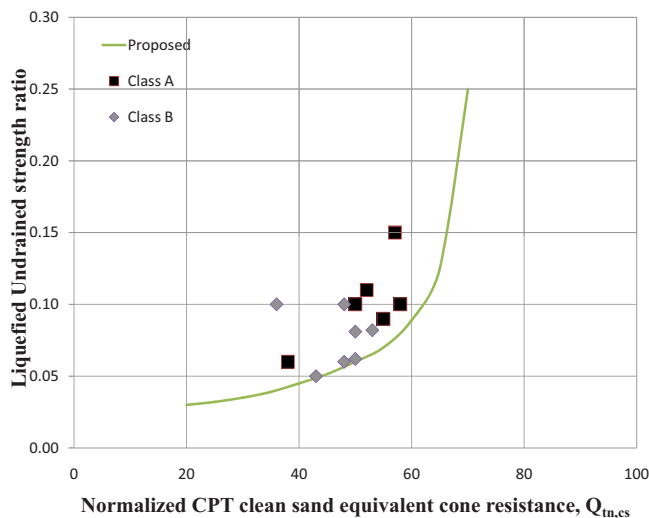


Fig. 7. Liquefied shear strength ratio and normalized CPT clean sand equivalent penetration resistance from Classes A and B flow liquefaction failure case histories

drained shear strength will typically exceed the drained shear strength, although cavitation can limit the full value of the undrained strength. The strength ratio in terms of drained shear strength (in simple shear) can be represented as

$$\tau/\sigma'_{vo} = \tan \phi' \quad (9)$$

The drained strength ratio in triaxial compression can be larger than defined by Eq. (9). Hence, for soils that are strain hardening in undrained shear, i.e., where $Q_{m,cs} > 70$, a conservative low estimate of the undrained strength ratio is about 0.4–0.5.

Fig. 7 shows the best estimate values for the liquefied strength ratios and mean CPT clean sand equivalent penetration resistance values for Classes A and B case histories. The more reliable CPT results from the case histories that are Class A are shown in large solid symbols and Class B by the large shaded symbols. Classes C, D, and E case histories are not included in Fig. 7 because of the lack of reliability and uncertainty. However, their assigned values are included in Table 2 for completeness. Based on the observation that no case history, with reliable measured CPT results, had a mean clean sand equivalent normalized penetration resistance, $Q_{m,cs} > 70$ and the observation that most soils are strain hardening (i.e., not susceptible to strength loss) in undrained shear when $Q_{m,cs} > 70$ with $\tau/\sigma'_{vo} \sim 0.4$, a proposed lower bound relationship is included in Fig. 7. Based on the above observations, the proposed relationship trends toward $s_{u(liq)}/\sigma'_{vo} = 0.4$ at $Q_{m,cs} = 70$.

The proposed single relationship can be represented by the following approximate equation: when $Q_{m,cs} \leq 70$

$$s_{u(liq)}/\sigma'_{vo} = [0.02199 - 0.0003124Q_{m,cs}] / [1 - 0.02676Q_{m,cs} + 0.0001783(Q_{m,cs})^2] \quad (10)$$

where $0.03 \leq s_{u(liq)}/\sigma'_{vo} \leq \tan \phi'$.

Unlike Seed and Harder (1990) and Olson and Stark (2002) a single relationship is recommended to conservatively capture the more reliable case-history data combined with the observation that most soils are strain hardening when $Q_{m,cs} > 70$ and therefore not susceptible to flow liquefaction. Table 2 presents the possible range of values for $s_{u(liq)}/\sigma'_{vo}$ and the proposed relationship captures almost all the range for the more reliable Classes A and B

case histories. The proposed relationship avoids the possibility of extrapolating beyond the available case-history data, since the proposed relationship trends toward the drained shear strength ratio represented by $\tan \phi'$. A conservative, essentially lower bound, relationship was selected to capture much of the variability in the back-calculated liquefied shear strength values from the case histories and to recognize the need for caution in soils where $Q_{m,cs} < 70$.

The proposed relationship can be conservatively low in sensitive clays, where the remolded shear strength ratio $s_{u(r)}/\sigma'_{vo}$ can be defined by

$$s_{u(r)}/\sigma'_{vo} = f_s/\sigma'_{vo} = (F_r Q_m)/100 \quad (11)$$

Eq. (11) is based on the observation that the remolded shear strength for most clay soils is approximately equal to the CPT sleeve friction, f_s (Robertson 2009b).

When the proposed relationship is applied to all CPT results within a sounding, it is recommended that the average value of liquefied shear strength within a noninterlayered soil deposit that is considered to be susceptible to strength loss should be applied for stability analyses, since the relationship was based on average CPT values within noninterlayered deposits from case histories. Hence, the variability within one soil type is captured, as illustrated by the range of CPT results for each case history shown in Fig. 5. To avoid excessive conservatism at low confining stress a lower bound value of $s_{u(liq)} = 1$ kPa should be assumed.

Idriss and Boulanger (2007) suggested an alternate more conservative relationship and included a relationship for conditions where the effects of void redistribution could be significant, although little evidence was presented to support this and little guidance was provided to evaluate when this might occur. The Idriss and Boulanger (2007) relationship is inconsistent with the observation that no case histories exist where $Q_{m,cs} > 70$. The LSFD case history may provide some guidance, since it is possible that the more dense sand layers were not susceptible to strain softening (i.e., flow liquefaction) initially but may have experienced some strain softening due to either void redistribution and/or particle intermixing after the earthquake. The representative mean CPT values in the weaker sand layers for the LSFD case history were $Q_m = 35$, $F_r = 2.3$, and $Q_{m,cs} = 90$. Many of the sand layers were more dense with even higher values of Q_m and $Q_{m,cs}$. Given the initial dense state of these sand layers it is likely that strength loss was confined primarily to the weaker sandy silt layers. The CPT results presented in Fig. 2 show that much of the zone where strength loss was considered to have taken place was composed primarily of the weaker sand silt. Although the denser sand layers may not have experienced strength loss, the resulting mixing of the soils as deformations became large may have resulted in the slightly higher back-calculated average strength ratio. In cases where less permeable layers may inhibit pore pressure dissipation and where void redistribution could occur, a more conservative estimate may be appropriate, and for high risk projects, more detailed field and analytical studies should be used.

Summary

An update of the CPT-based criteria to evaluate the susceptibility to flow liquefaction and the liquefied strength ratio based on case histories has been presented. The criteria of $Q_{m,cs} \leq 70$ can be used as a conservative screening method to evaluate if a

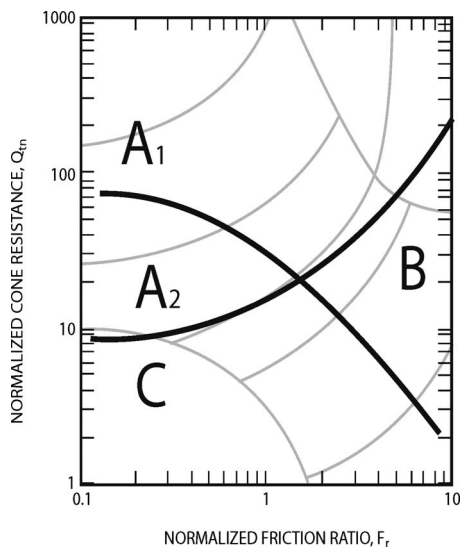


Fig. 8. CPT SBT chart for liquefaction and cyclic softening potential: *cohesionless soils* (A_1 and A_2)—evaluate potential behavior using CPT-based case-history liquefaction correlations. A_1 : cyclic liquefaction possible depending on level and duration of cyclic loading. A_2 : cyclic liquefaction and flow liquefaction possible depending on loading and ground geometry. *Cohesive soils* (B and C)—evaluate potential behavior based on in situ or laboratory test measurements or estimates of monotonic and cyclic undrained shear strengths. B : cyclic softening possible depending on level and duration of cyclic loading. C : cyclic softening and flow liquefaction possible depending on soil sensitivity, loading, and ground geometry.

soil is susceptible to strain softening in undrained shear and, hence, susceptible to flow liquefaction. The recommended correction factors to derive the clean sand equivalent penetration resistance are supported by the general concepts in critical state soil mechanics.

The case histories indicate that very young, very loose, non-plastic or low-plastic soils tend to be more susceptible to significant and rapid strength loss than older, denser, and/or more plastic soils. Ladd et al. (1977) and Leroueil and Hight (2003) showed that soils with high plasticity tend to be more ductile than soils of low plasticity. Low plastic, highly sensitive, fine-grained soils that have a shear strain at peak undrained shear strength less than about 2% and a rapid loss of strength are more likely to experience rapid strain softening and flow liquefaction than more plastic soils.

Robertson (2009c) presented a summary of the CPT SBT Q_m - F_r chart to identify zones of potential liquefaction and/or cyclic softening as shown in Fig. 8 that can be used as a guide for the choice of engineering procedures to be used in evaluating potential liquefaction and strength loss in different types of soils. The boundary between Zones A_1 and A_2 and Zones B and C can be approximated by the CPT SBT $I_c = 2.60$. The boundary between Zones A_1 and B and Zones A_2 and C can be defined by $Q_{m,cs} = 70$. Zones A_1 and A_2 correspond to cohesionless, predominately sandlike soils for which it is appropriate to use existing CPT case-history based cyclic liquefaction correlations (e.g., Youd et al. 2001; Robertson and Wride 1998). The soils in Zones A_1 and A_2 are susceptible to cyclic liquefaction, while the looser soils in Zone A_2 are more susceptible to strength loss and flow liquefaction. Zones B and C correspond to fine-grained, predominately claylike soils for which it is more appropriate to use pro-

cedures similar to, or modified from, those used to evaluate the undrained shear strength of clays (e.g., field vane tests, CPT, and shear strength tests on high-quality thin-walled tube samples). The soils in Zones B and C are susceptible to cyclic softening (e.g., accumulation of strains if the peak seismic/cyclic stresses are sufficiently large), but the softer soils in Zone C can be more sensitive and susceptible to potential strength loss and possible flow liquefaction. For moderate to high risk projects, an undisturbed sampling of soils in Zones B and C is recommended to determine the soil response, since soils in these zones are generally more suitable for conventional high-quality sampling and laboratory testing. High-quality samples are required, since the peak undrained shear strength and the strain to peak strength are sensitive to soil disturbance (Leroueil and Hight 2003). For low risk projects, disturbed samples should be obtained for soils in Zones B and C to estimate if the soils will respond either more sandlike or claylike (Idriss and Boulanger 2004), and evaluate sensitivity (Leroueil et al. 1983), based on Atterberg limits and water content.

A lower bound relationship between the liquefied shear strength and clean sand equivalent normalized penetration resistance is proposed that avoids the need to extrapolate beyond the case-history database. In cases where less permeable layers may inhibit pore pressure dissipation and where void redistribution could occur, a more conservative estimate may be appropriate, and for high risk projects, more detailed field and analytical studies should be carried out. When the proposed relationship is applied to all CPT results within a noninterlayered soil deposit, it is recommended that the average value of liquefied shear strength should be applied for stability analyses, since the relationship was based on average CPT values within noninterlayered deposits from the case histories. To avoid excessive conservatism at low confining stress, a lower bound value of $s_{u(liq)} = 1$ kPa should be assumed.

The case histories have shown that when significant strength loss occurs in critical sections of a soil structure, failures are often rapid, occur with little warning, and the resulting deformations are often very large. Experience has also shown that the trigger events can be very small. In general, it is often prudent to assume that triggering will occur if the soils are susceptible to strength loss. Hence, the design for high risk soil structures should be carried out with caution. In general the emphasis in design is primarily on the evaluation of susceptibility and the resulting liquefied shear strength.

The CPT is a useful in situ test that can provide continuous estimates of the potential for flow liquefaction. However, the CPT-based approach is a simplified method that should be used appropriately depending on the risk of the project. For low risk projects, the CPT-based method is appropriate when combined with selective samples to confirm the soil type as well as conservative estimates of soil response. For moderate risk projects, the CPT-based method should be combined with appropriate additional in situ testing, as well as selected undisturbed sampling and laboratory testing, to confirm soil response. A thin-walled tube sampling is generally applicable to fine-grained soils in Zones B and C . For high risk projects, the CPT-based method should be used as an initial screening to identify the extent and nature of potential problems followed by additional in situ testing and appropriate laboratory testing on high-quality samples. An advanced numerical modeling is appropriate for high risk projects where initial screening indicates a need.

Acknowledgments

This research could not have been carried out without the support, encouragement, and input from John Gregg, Kelly Cabal, and other staff at Gregg Drilling and Testing, Inc.

References

- Ahmadi, M. M., and Robertson, P. K. (2005). "Thin layer effects on the CPT qc measurement." *Can. Geotech. J.*, 42(5), 1302–1317.
- Been, K., Crooks, J. H. A., Becker, D. E., and Jefferies, M. G. (1986). "The cone penetration test in sands: Part 1. State parameter interpretation." *Geotechnique*, 36(2), 239–249.
- Been, K., and Jefferies, M. G. (1985). "A state parameter for sands." *Geotechnique*, 35(2), 99–112.
- Campanella, R. G., Gillespie, D., and Robertson, P. K. (1982). "Pore pressures during cone penetration testing." *Proc., 2nd European Symp. on Penetration Testing, ESPOT II*, Balkema, Rotterdam, The Netherlands, 507–512.
- Casagrande, A. (1940). "Characteristics of cohesionless soils affecting the stability of slopes and earth fills." *Contributions to soil mechanics*, Boston Society of Civil Engineers, 257–276.
- Castro, G. (1969). "Liquefaction of sands." *Harvard soil mechanics series*, Vol. 81, Harvard University, Cambridge, Mass.
- Castro, G. (1975). "Liquefaction and cyclic mobility of saturated sands." *J. Geotech. Engrg. Div.*, 101(6), 551–569.
- Castro, G., Keller, T. O., and Boynton, S. S. (1989). "Re-evaluation of the Lower San Fernando Dam. Report 1: An investigation of the February 9, 1971 slide." *U.S. Army Corps of Engineers Contract Rep. No. GL-89-2*, U.S. Army Corps of Engineers Waterways Experiment Station, Vicksburg, Miss.
- Castro, G., Seed, R. B., Keller, T. O., and Seed, H. B. (1992). "Steady state strength analysis of lower San Fernando Dam slide." *J. Geotech. Engrg.*, 118(3), 406–427.
- Cetin, K. O., and Isik, N. S. (2007). "Probabilistic assessment of stress normalization for CPT data." *J. Geotech. Geoenviron. Eng.*, 133(7), 887–897.
- Cetin, K. O., and Ozan, C. (2009). "CPT-based probabilistic soil characterization and classification." *J. Geotech. Geoenviron. Eng.*, 135(1), 84–107.
- Davies, M. P., Dawson, B. D., and Chin, B. G. (1998). "Static liquefaction slump of mine tailings—A case history." *Proc., 51st Canadian Geotechnical Conf.*, BiTech Publishers, Vancouver, BC, Canada, 123–131.
- Davis, A. P., Poulos, S. J., and Castro, G. (1988). "Strengths back figured from liquefaction case histories." *Proc., 2nd Int. Conf. on Case Histories in Geotechnical Engineering*, University of Missouri-Rolla, Rolla, Mo., 1693–1701.
- Finn, W. D. L. (1981). "Liquefaction potential: Developments since 1976." *Proc., 1st Int. Conf. on Recent Advances in Geotechnical Earthquake Engineering and Soil Dynamics*, S. Prakash, ed., University of Missouri-Rolla, Rolla, Mo., 655–681.
- Gilstrap, S. D., and Youd, T. L. (1998). "CPT based liquefaction resistance analyses evaluated using case histories." *Technical Rep. No. CEG-98-01*, Dept. of Civil and Environmental Engineering, Brigham Young Univ., Provo, Utah.
- Idriss, I. M., and Boulanger, R. W. (2004). "Semi-empirical procedures for evaluating liquefaction potential during earthquakes." *Proc., 11th Int. Conf. on Soil Dynamics and Earthquake Engineering*, Stallion Press, Tokyo, 32–56.
- Idriss, I. M., and Boulanger, R. W. (2007). "SPT- and CPT-based relationships for residual shear strength of liquefied soils." *Proc., 4th Int. Conf. on Earthquake Geotechnical Engineering*, K. D. Pitilakis, ed., Springer, New York, 1–22.
- Ishihara, K. (1993). "Liquefaction and flow failure during earthquakes." *Geotechnique*, 43(3), 351–451.
- Jefferies, M. G., and Been, K. (2006). *Soil liquefaction—A critical state approach*, Taylor and Francis, London.
- Jefferies, M. G., and Davies, M. O. (1991). "Soil classification by the cone penetration test: Discussion." *Can. Geotech. J.*, 28(1), 173–176.
- Jefferies, M. G., and Davies, M. P. (1993). "Use of CPTU to estimate equivalent SPT N_{60} ." *Geotech. Test. J.*, 16(4), 458–468.
- Konrad, J.-M., and Watts, B. D. (1995). "Undrained shear strength for liquefaction flow failure analysis." *Can. Geotech. J.*, 32, 783–794.
- Ladd, C. C., Foott, R., Ishihara, K., Schlosser, F., and Poulos, H. G. (1977). "Stress-deformation and strength characteristics: State-of-the-art-report." *Proc., 9th Int. Conf. on Soil Mechanics and Foundation Engineering*, Balkema, Tokyo, 421–94.
- Leroueil, S., and Hight, D. W. (2003). "Behaviour and properties of natural soils and rocks." *Proc., Int. Conf. on Characterization and Engineering Properties of Natural Soils*, Swets and Zeitlinger, Singapore, 29–253.
- Leroueil, S., Tavenas, F., and Le Bihan, J. P. (1983). "Propriétés caractéristiques des argiles de l'est Canada." *Can. Geotech. J.*, 17(4), 591–602.
- Lunne, T., Robertson, P. K., and Powell, J. J. M. (1997). *Cone penetration testing in geotechnical practice*, Blackie Academic, E & FN Spon/Routledge, New York.
- Moss, R. E. S., Seed, R. B., and Olsen, R. S. (2006). "Normalizing the CPT for overburden stress." *J. Geotech. Geoenviron. Eng.*, 132(3), 378–387.
- Olsen, R. S., and Malone, P. G. (1988). "Soil classification and site characterization using the cone penetrometer test." *Penetration Testing 1988, ISOPT-1*, J. De Ruiter, ed., Balkema, Rotterdam, The Netherlands, 887–893.
- Olson, S. M. (2001). "Liquefaction analysis of level and sloping ground using field case histories and penetration resistance." Ph.D. thesis, Univ. of Illinois at Urbana-Champaign, Urbana, Ill.
- Olson, S. M., and Stark, T. D. (2002). "Liquefied strength ratio from liquefaction flow failure case histories." *Can. Geotech. J.*, 39, 629–647.
- Olson, S. M., and Stark, T. D. (2003). "Yield strength ratio and liquefaction analysis of slopes and embankments." *J. Geotech. Geoenviron. Eng.*, 129(8), 727–737.
- Plewes, H. D., Davies, M. P., and Jefferies, M. G. (1992). "CPT based screening procedure for evaluating liquefaction susceptibility." *Proc., 45th Canadian Geotechnical Conf.*, Vol. 4, BiTech Publishers, Vancouver, BC, Canada, 1–9.
- Popescu, R., Prevost, J. H., and Deodatis, G. (1997). "Effects of spatial variability on soil liquefaction: Some design recommendations." *Geotechnique*, 47(5), 1019–1036.
- Poulos, S. J., Castro, G., and France, W. (1985). "Liquefaction evaluation procedure." *J. Geotech. Engrg. Div.*, 111(6), 772–792.
- Robertson, P. K. (1990). "Soil classification using the cone penetration test." *Can. Geotech. J.*, 27(1), 151–158.
- Robertson, P. K. (1999). "Estimation of minimum undrained shear strength for flow liquefaction using the CPT." *Proc., 2nd Int. Conf. on Earthquake Geotechnical Engineering*, Balkema, Rotterdam, The Netherlands.
- Robertson, P. K. (2009a). "Discussion of 'CPT-based probabilistic soil characterization and classification' by K. Onder Cetin and Cem Ozan." *J. Geotech. Geoenviron. Eng.*, 135(1), 84–107.
- Robertson, P. K. (2009b). "Interpretation of cone penetration tests—A unified approach." *Can. Geotech. J.*, 46, 1337–1355.
- Robertson, P. K. (2009c). "Performance based earthquake design using the CPT." *Proc., IS Tokyo Conf.*, CRC Press/Balkema, Taylor & Francis Group, Tokyo.
- Robertson, P. K. (2010). "Estimating in situ state parameter in sandy soils from the CPT." *Proc., 2nd Int. Symp. of the Cone Penetration Test, CPT '10*, Omnipress Publishers, Madison, Wis.

- Robertson, P. K., et al. (2000). "The Canadian liquefaction experiment: An overview." *Can. Geotech. J.*, 37, 499–504.
- Robertson, P. K., and Fear, C. E. (1995). "Liquefaction of sands and its evaluation." *IS-Tokyo '95, Proc., 1st Int. Conf. on Earthquake Geotechnical Engineering*, K. Ishihara, ed., Balkema, Rotterdam, The Netherlands, 1253–1289.
- Robertson, P. K., and Wride, C. E. (1998). "Evaluating cyclic liquefaction potential using the CPT." *Can. Geotech. J.*, 35(3), 442–459.
- Schofield, A., and Wroth, C. P. (1968). *Critical state soil mechanics*, McGraw-Hill, London.
- Seed, H. B. (1979). "Soil liquefaction and cyclic mobility evaluation for level ground during earthquakes." *J. Geotech. Engrg. Div.*, 105(2), 201–255.
- Seed, H. B. (1987). "Design problems in soil liquefaction." *J. Geotech. Engrg. Div.*, 113(8), 827–845.
- Seed, H. B., and Harder, L. F. (1990). "SPT-based analysis of cyclic pore pressure generation and undrained residual strength." *Proc., Seed Memorial Symp.*, BiTech Publishers, Vancouver, BC, Canada, 351–376.
- Seed, H. B., Lee, K. L., Idriss, I. M., and Makdisi, F. (1973). "Analysis of the slides in the San Fernando Dams during the earthquake of Feb. 9, 1971." *Earthquake Engineering Research Center Rep. No. EERC 73-2*, Univ. of California, Berkeley, Calif.
- Seed, H. B., Seed, R. B., Harder, L. F., and Jong, H.-L. (1989). "Reevaluation of the lower San Fernando Dam: Report 2, examination of the post-earthquake slide of February 9, 1971." *U.S. Army Corps of Engineers Contract Rep. No. GL-89-2*, U.S. Army Corps of Engineers Waterways Experiment Station, Vicksburg, Miss.
- Shuttle, D. A., and Cuning, J. (2007). "Liquefaction potential of silts from CPTu." *Can. Geotech. J.*, 44, 1–19.
- Silvis, F., and de Groot, D. (1995). "Flow slides in the Netherlands: Experience and engineering practice." *Can. Geotech. J.*, 32, 1086–1092.
- Stark, T. D., and Mesri, G. (1992). "Undrained shear strength of sands for stability analysis." *J. Geotech. Engrg. Div.*, 118(11), 1727–1747.
- Terzaghi, K., and Peck, R. B. (1967). *Soil mechanics in engineering practice*, 1st Ed., Wiley, New York.
- Wride, C. E., McRoberts, E. C., and Robertson, P. K. (1999). "Reconsideration of case histories for estimating undrained shear strength in sandy soils." *Can. Geotech. J.*, 36, 907–933.
- Yoshimi, Y., Richart, F. E., Prakash, S., Balkan, D. D., and Ilyichev, Y. L. (1977). "Soil dynamics and its application to foundation engineering." *Proc., 9th Int. Conf. on Soil Mechanics and Foundation Engineering*, Balkema, Tokyo, 605–650.
- Yoshimine, M., Robertson, P. K., and Wride, C. E. (1999). "Undrained shear strength of clean sands to trigger flow liquefaction." *Can. Geotech. J.*, 36, 891–906.
- Youd, T. L., et al. (2001). "Liquefaction resistance of soils: Summary report from the 1996 NCEER and 1998 NCEER/NSF workshops on evaluation of liquefaction resistance of soils." *J. Geotech. Geoenviron. Eng.*, 127(4), 297–313.
- Zhang, G., Robertson, P. K., and Brachman, R. W. I. (2002). "Estimating liquefaction induced ground settlements from CPT for level ground." *Can. Geotech. J.*, 39(5), 1168–1180.